NATIONAL ADVISORY COMMITTEE FOR AERONAUTICS

TECHNICAL NOTE 2347

EFFECT OF ASPECT RATIO AND SWEEPBACK ON THE LOW-SPEED LATERAL CONTROL CHARACTERISTICS OF UNTAPERED LOW-ASPECT-RATIO WINGS EQUIPPED WITH RETRACTABLE AILERONS

By Jack Fischel and John R. Hagerman

Langley Aeronautical Laboratory
Langley Field, Va.

Washington
May 1951

NATIONAL ADVISORY COMMITTEE FOR AERONAUTICS

TECHNICAL NOTE 2347

EFFECT OF ASPECT RATIO AND SWEEPBACK ON THE LOW-SPEED LATERAL CONTROL CHARACTERISTICS OF UNTAPERED LOW-ASPECT-RATIO WINGS EQUIPPED WITH RETRACTABLE AILERONS

By Jack Fischel and John R. Hagerman

SUMMARY

A low-speed wind-tunnel investigation was made to determine the lateral control characteristics of three untapered unswept wings of aspect ratio 1.13, 2.13, and 4.13 and an untapered 45° sweptback wing of aspect ratio 2.09 equipped with 0.60-semispan retractable ailerons having various projections. Each of the wings had an NACA 64A010 airfoil section and had the ailerons mounted at the 0.70-chord station. The continuous-span aileron investigated on the unswept wings spanned the outboard stations of each wing; whereas the plain (continuous span) and stepped (segmented) retractable ailerons investigated on the sweptback wing were located at various spanwise stations and were tested with and without simulated actuating arms.

At equal aileron projections, the rolling effectiveness of the retractable ailerons increased with increase in aspect ratio of the unswept wings and decreased with increase in wing sweepback; however, the rolling velocities of the four wings are estimated to be approximately equal for a given wing area at the maximum aileron projection investigated. The effectiveness of plain retractable ailerons on the sweptback wing generally increased when the spanwise location of the aileron was moved inboard; whereas the effectiveness of stepped retractable ailerons on the same wing generally increased at low and moderate angles of attack when their spanwise location was moved outboard.

INTRODUCTION

The National Advisory Committee for Aeronautics is currently investigating the applicability of various types of lateral-control devices to wings having plan forms suitable for flight at high-subsonic or

transonic speeds. Among the more promising types of lateral-control devices being investigated are spoiler ailerons. Previous spoiler-aileron investigations made with unswept and swept wings of moderate and high aspect ratio (references 1 to 7 and unpublished data) indicate some of the beneficial effects that are obtained with spoiler ailerons, such as: increase in rolling moment with increase in Mach number; increase in rolling effectiveness with increase in lift-flap deflection; generally favorable yawing moments; practicable use of full-span flaps with spoiler ailerons; and smaller wing twisting moments than flap ailerons and hence higher reversal speeds with spoiler ailerons (reference 8). In addition, spoiler ailerons provide low stick forces; and, in the investigation of reference 2, no appreciable effects on the hinge-moment characteristics were observed with changes in Mach number for the spoiler aileron.

The present investigation was made at low speed in the Langley 300 MPH 7- by 10-foot tunnel to determine the lateral control characteristics of four untapered low-aspect-ratio wings equipped with spoiler ailerons (retractable ailerons). Three of the wings investigated were unswept, had aspect ratios of 1.13, 2.13, and 4.13, and were tested with 0.60-semispan retractable ailerons at the 0.70-wing-chord station. The other wing investigated had 45° sweepback and an aspect ratio of 2.09 and was tested with 0.60-semispan plain and stepped retractable ailerons at the 0.70-wing-chord station. Each of the wings was tested through an angle-of-attack range at various aileron projections. In addition, the effects of aileron spanwise location and aileron actuating arms on the lateral control characteristics of the sweptback wing were determined for both the plain- and stepped-retractable-aileron configurations.

SYMBOLS

The forces and moments measured on the wings are presented about the wind axes which, for the conditions of these tests (zero yaw), correspond to the stability axes. These axes have their origin at the intersection of the chord plane and the 25-percent-chord station of the mean aerodynamic chord (figs. 1 and 2).

The symbols used in the presentation of results are as follows:

C_L lift coefficient (Lift/qS)

C_D drag coefficient (Drag/qS)

C_m pitching-moment coefficient ($M/qS\bar{c}$)

C_l rolling-moment coefficient (L/qSb)

C_n	yawing-moment coefficient (N/qSb)
C_{l_p}	damping-in-roll coefficient; that is, rate of change of rolling-moment coefficient with wing-tip helix angle $\left(\partial C_l \Big/ \partial \frac{pb}{2V}\right)$
$pb/2V$	wing-tip helix angle, radians
M	pitching moment of model about $0.25\bar{c}$, foot-pounds
L	rolling moment due to aileron about x-axis, foot-pounds
N	yawing moment due to aileron about z-axis, foot-pounds
q	dynamic pressure, pounds per square foot $\left(\frac{1}{2}\rho V^2\right)$
S	wing area, square feet (see table I)
b	span of model measured normal to plane of symmetry, feet (see table I)
b_a	span of retractable aileron measured normal to plane of symmetry, feet
A	aspect ratio of wing (b^2/S) (see table I)
$\bar{c}$	wing mean aerodynamic chord (M.A.C.), feet $\left(\frac{2}{S}\int_0^{b/2} c^2 dy\right)$ (see table I)
c	local wing chord measured parallel to plane of symmetry at $\alpha = 0^\circ$, feet
y	lateral distance from plane of symmetry, feet
y_i	lateral distance from plane of symmetry to inboard end of retractable aileron, feet
y_o	lateral distance from plane of symmetry to outboard end of retractable aileron, feet
p	rolling velocity, radians per second
V	free-stream velocity, feet per second
ρ	mass density of air, slugs per cubic foot

α angle of attack of wing with respect to chord plane of model, degrees

Λ angle of sweepback, degrees

R Reynolds number

$C_{L_\alpha} = \frac{\partial C_L}{\partial \alpha}$

The rolling-moment and yawing-moment coefficients presented herein represent the aerodynamic effects that occur on the complete wing as a result of the projection of a retractable aileron on the right semispan of the wing.

APPARATUS AND MODELS

Each of the four wing models investigated was tested while it was mounted horizontally in the Langley 300 MPH 7- by 10-foot tunnel on a single strut which, in turn, was mounted on a six-component balance system in such a manner that all the forces and moments acting on the model could be measured.

The four untapered wing models investigated were constructed according to the plan-form dimensions shown in figures 1 and 2 and table I. The wings had neither twist nor dihedral, and the airfoil sections normal to the leading edge of each wing had an NACA 64A010 profile. Each model was fabricated by means of a sandwich type of construction consisting of a laminated mahogany core enclosed in a covering composed of $\frac{1}{32}$-inch sheet aluminum glued between sheets of $\frac{1}{32}$-inch fir.

One of the two configurations of retractable ailerons investigated consisted of plain, $0.60\frac{b}{2}$, continuous-span, retractable ailerons attached to the upper surface of the right wing along the 0.70c line of each wing model (figs. 1 and 2). The other configuration consisted of six individual retractable-aileron segments, each having a span of $0.10\frac{b}{2}$ and a total aileron span of $0.60\frac{b}{2}$, attached to the upper surface of the right wing of the 45° sweptback-wing model in a stepped fashion with the span of each segment normal to the plane of symmetry (fig. 2). The midpoint of each stepped-retractable-aileron segment was on the 0.70c line of the sweptback wing. Several ailerons, each having different projections, were used in tests of the two retractable-aileron configurations,

and each aileron was prefabricated of aluminum angle and was mounted in such a manner that the front face of each aileron was normal to the wing surface (figs. 1 and 2). On the unswept-wing models, the ailerons were mounted on the outboard portions of the wing; whereas, on the 45° sweptback-wing model, the spanwise location of the ailerons was varied during the investigation. To distinguish clearly between the two aileron configurations investigated on the sweptback wing, they are referred to herein as the "plain retractable aileron" and the "stepped retractable aileron."

The simulated actuating arms tested on the sweptback-wing model in conjunction with $0.60\frac{b}{2}$ plain and stepped retractable ailerons having projections of -0.08c and various spanwise locations are shown in figure 3. The arms were constructed of thin solid triangular-shaped pieces of aluminum, each of which had a chord of 10 percent of the wing chord parallel to the plane of the actuating arm and a maximum height of 0.08c. The actuating arms were mounted normal to the wing surface and to the front face of each aileron at spanwise intervals of $0.10\frac{b}{2}$ for the plain retractable aileron and at the inboard and outboard ends of each stepped-retractable-aileron segment (fig. 3).

TESTS

All the tests were performed in the Langley 300 MPH 7- by 10-foot tunnel at an average dynamic pressure of 99 pounds per square foot, which corresponds to a Mach number of 0.26 and to Reynolds numbers, based on the mean aerodynamic chord of each wing model, shown in the following table:

Aspect ratio, A	Sweep, Λ (deg)	Mean aerodynamic chord, $\bar{c}$ (ft)	Reynolds number, R
4.13	0	1.221	2.2×10^6
2.13	0	1.714	3.1
1.13	0	2.409	4.4
2.09	45	1.718	3.1

Tests were conducted through an angle-of-attack range from -6° to the angle of wing stall for each of the retractable-aileron configurations.

CORRECTIONS

Jet-boundary (induced upwash) corrections have been applied to the angle-of-attack and drag data according to the methods of reference 9. Blockage corrections have been applied to the data by the methods of reference 10. Corrections have also been applied to the data to account for the model-support-strut tares.

RESULTS AND DISCUSSION

Wing Aerodynamic Characteristics

The lift, drag, and pitching-moment characteristics of the four plain wing models used in the present investigation are presented in figure 4. Because the data for the unswept wings have been reported and discussed in reference 11, these data are not discussed herein. The data of figure 4 show, however, that the maximum lift coefficient of the sweptback wing was larger than that of any of the unswept wings investigated. Moreover, the value of lift-curve slope C_{L_α} of the sweptback wing was slightly less than that of the unswept wing of comparable aspect ratio and could be accurately predicted by theory.

Lateral Control Characteristics for Unswept Wings

The rolling-moment and yawing-moment characteristics over the angle-of-attack range of each of the unswept-wing models equipped with $0.60\frac{b}{2}$ outboard retractable ailerons at various projections are presented in figures 5 to 7. Cross plots of the rolling-moment data of figures 5 to 7 plotted as a function of retractable-aileron projection and wing aspect ratio are presented in figures 8 and 9, respectively.

Effect of aileron projection.- The values of C_l produced by projection of the retractable ailerons on the unswept wings of aspect ratios 4.13 and 2.13 generally decreased with increase in angle of attack up to the stall angle; however, the values of C_l produced by projection of the retractable ailerons on the unswept wing of aspect ratio 1.13 varied erratically with change in angle of attack and became completely

reversed for various projections above angles of attack of 18° to 24° (figs. 5 to 7). This angle-of-attack range of aileron reversal for the wing of aspect ratio 1.13 corresponds to the range of separated flow over the plain wing, where a partial flow recovery probably is caused by the tip vortex on the wing rearward of the aileron. (See fig. 4.)

Each of the unswept wings exhibited a region of zero or reversed aileron effectiveness for small aileron projections, and the aileron-projection range for this phenomenon decreased with increase in wing aspect ratio (figs. 5 to 8). At larger aileron projections, the variation of C_l with retractable-aileron projection was generally fairly linear for each of the wings (fig. 8). Because the data of references 2 and 3 indicate that an increase in aileron effectiveness with increase in Mach number may be expected over the entire projection range for this aileron configuration, particularly for small aileron projections, the aforementioned ineffective region of roll for small aileron projections is believed to be materially alleviated in flight at high-subsonic speeds. For the wing of aspect ratio 1.13, it is rather dubious that this ineffective region of roll would be completely eliminated by increases in Mach number, but on the other wings, rolling-moment coefficients would probably be more linear with retractable-aileron projection. Other means of alleviating the ineffectiveness of the retractable aileron at small projections are also available - such as slotting the wing immediately behind the aileron and thereby making it a plug aileron (reference 4).

The yawing moments produced by projection of the retractable ailerons on the three unswept wings were generally favorable (having the same sign as the rolling moments) and increased linearly except at small projections with increase in aileron projection (figs. 5 to 7). The values of C_n decreased with increase in α on the wings of aspect ratios 4.13 and 2.13 but increased with increase in α up to $\alpha \approx 20°$ on the wing of aspect ratio 1.13.

Effect of wing aspect ratio.- Larger values of C_l were produced at given aileron projections as the wing aspect ratio increased, and this increase in C_l with increase in aspect ratio was almost linear but was largest at low lift coefficients (fig. 9, also figs. 5 to 8). Also, as discussed in the preceding section, increase in wing aspect ratio of the unswept wings reduced the aileron-projection range of zero or reversed aileron effectiveness encountered at small projections (figs. 5 to 8).

At small values of α or C_L, more favorable values of C_n were produced by given aileron projections as the wing aspect ratio was increased, but at large values of α or C_L, an opposite effect occurred

(figs. 5 to 7). In addition, the ratio of C_n to C_l tended to decrease with increase in wing aspect ratio, particularly at large values of α or C_L.

Lateral Control Characteristics for 45° Sweptback Wing

The rolling-moment and yawing-moment characteristics over the angle-of-attack range of the 45° sweptback wing of aspect ratio 2.09 equipped with $0.60\frac{b}{2}$ plain and stepped retractable ailerons located from $0.20\frac{b}{2}$ to $0.80\frac{b}{2}$ and having various projections are presented in figures 10 and 11. The rolling-moment data of figures 10 and 11 are shown cross-plotted against aileron projection in figure 12. The effects of aileron spanwise location and of aileron actuating arms on the lateral control characteristics of the sweptback wing equipped with $0.60\frac{b}{2}$ plain and stepped retractable ailerons having a projection of -0.08c are shown in figures 13 and 14, respectively.

Effect of aileron projection.- The values of C_l produced by various projections of the plain and stepped retractable ailerons varied non-linearly over the angle-of-attack range and, with the exception of a range of small projections, varied almost linearly with aileron projection (figs. 10 to 12). The region of aileron ineffectiveness or reversed effectiveness, which occurred to a slight extent as noted in figure 12 for small projections for the plain retractable aileron, was also observed on the unswept wings but, as previously discussed, was found to be a low-speed phenomenon and should be alleviated at high-subsonic speeds (references 2 and 3). This effect of Mach number would thus be expected to provide for an almost linear variation of C_l with aileron projection at high-subsonic speeds, a phenomenon which has been noted in some unpublished data obtained on another sweptback-wing model at high-subsonic speeds.

The yawing moments produced by projection of both plain and stepped retractable ailerons were generally favorable at values of α below 18° and became less favorable with a further increase in α (figs. 10 and 11). With both retractable-aileron configurations, C_n increased almost linearly with aileron projection except at small projections.

Comparison of plain and stepped retractable ailerons.- Comparison of the data of figures 10 and 11 shows that the $0.60\frac{b}{2}$ plain retractable aileron located from $0.20\frac{b}{2}$ to $0.80\frac{b}{2}$ generally produced larger values

of C_l at small values of α and smaller values of C_l at large values of α than the stepped retractable aileron located at the same spanwise stations. Both ailerons had some effectiveness near the wing stall angle. At small aileron projections, the plain retractable aileron generally exhibited zero or reversed effectiveness; whereas the stepped retractable aileron always had positive effectiveness.

The plain retractable aileron generally produced larger (more favorable) values of C_n at various projections than did the stepped retractable aileron over the angle-of-attack range.

Effect of aileron spanwise location.- The values of rolling-moment coefficient produced by a $0.60\frac{b}{2}$ plain retractable aileron projected -0.08c generally increased appreciably as the aileron was moved inboard on the wing (fig. 13). This trend agrees with unpublished results obtained at low speed for a 51° sweptback wing of aspect ratio 3.1. The values of C_l produced by stepped retractable ailerons generally increased at low and moderate angles of attack when the ailerons were moved outboard on the wing (fig. 14). This trend at low and moderate values of α is opposite to that noted in an investigation of a 42° sweptback wing of aspect ratio 4.01 (reference 5) and in the investigation of the aforementioned 51° sweptback wing of aspect ratio 3.1. However, at very large angles of attack the values of C_l produced by stepped retractable ailerons decreased when the ailerons were moved outboard on the wing. This trend is in agreement with the data obtained on the other wings at very large values of α. Reasons for this discrepancy are unknown but it may be attributed to differences in wing geometry - particularly, in the wing aspect ratio.

In general, the inboard, $0.60\frac{b}{2}$, plain retractable aileron, which was the optimum configuration for the plain retractable aileron on the 45° sweptback wing, produced larger values of C_l over the angle-of-attack range of the wing model than did the optimum configuration for the stepped retractable aileron, which was the outboard stepped retractable aileron.

With either the plain- or stepped-retractable-aileron configuration, C_n generally decreased (became less favorable) as the $0.60\frac{b}{2}$ aileron was moved inboard on the wing, but C_n was generally larger for all plain retractable ailerons than for comparable stepped retractable ailerons. This decrease in C_n as the aileron moved inboard agrees with results obtained on the aforementioned 42° and 51° sweptback wings (reference 5 and unpublished data, respectively).

Effect of aileron actuating arms.- The addition of aileron actuating arms (fig. 3) to $0.60\frac{b}{2}$ plain and stepped retractable ailerons having a projection of -0.08c at each of three spanwise locations generally tended to increase the values of C_l produced by the ailerons alone over most of the angle-of-attack range, except at small angles of attack for the plain retractable aileron at the two inboard locations investigated (figs. 13 and 14). In general, the effects on C_l produced by the actuating arms were very small at low angles of attack, except with the stepped ailerons at the inboard location, but were appreciable at large angles of attack.

With the exception of the outboard stepped retractable aileron in the low angle-of-attack range, all aileron configurations exhibited slightly less favorable yawing-moment characteristics with aileron actuating arms on the wing than when the ailerons were tested alone on the wing (figs. 13 and 14).

Effect of wing sweep.- A comparison of the data obtained with outboard, $0.60\frac{b}{2}$ retractable ailerons on the unswept wing of aspect ratio 2.13 (figs. 6 and 8) with comparable data obtained with midsemispan, $0.60\frac{b}{2}$ plain and stepped retractable ailerons on the 45° sweptback wing of aspect ratio 2.09 (figs. 10 to 12) shows that the ailerons on both wings generally produced a linear variation of C_l with aileron projection over most of the aileron-projection range. At given values of lift coefficient, the retractable ailerons on the unswept wing generally were appreciably more effective than on the sweptback wing; however, because the wing stall occurred at larger values of α and C_l on the sweptback wing (fig. 4), this wing retained more of its aileron effectiveness to larger values of α, particularly with the stepped retractable ailerons, than did the unswept wing. The yawing moments produced by these ailerons on both wings generally exhibited the same trends with increase in angle of attack and aileron projection and, at given values of C_L, were slightly larger for the plain retractable aileron on the 45° sweptback wing than for the retractable aileron on the unswept wing.

The data of references 1 and 12 show that the outboard portions of unswept wings are the most effective spanwise locations for both spoiler and flap controls, respectively; however, the data of reference 5 and unpublished data obtained on a 51° sweptback wing of aspect ratio 3.1, as well as the present data (figs. 13 and 14), show that aileron configuration and wing geometry influence the most effective spanwise location of spoiler controls on swept wings. Therefore, a comparison of the effectiveness of spoiler ailerons on unswept and swept wings should be made for the optimum aileron configuration on each wing. Accordingly,

a comparison of the data of figure 6 with the data of figure 14 shows that larger values of C_l were produced by the optimum retractable-aileron configuration on the unswept wing than by the optimum stepped-retractable-aileron configuration on the sweptback wing. At low lift coefficients the retractable aileron on the unswept wing produced larger values of C_l than the optimum plain-retractable-aileron configuration on the sweptback wing, but at large lift coefficients (or angles of attack greater than about 7°) an opposite effect was generally obtained. (See figs. 6 and 13.) The yawing moments produced by these retractable-aileron configurations exhibited the same trends with increase in α, but the aileron on the unswept wing generally produced larger (more favorable) values of C_n than the optimum configuration of plain retractable aileron and smaller values of C_n than the optimum configuration of stepped retractable aileron on the sweptback wing at comparable values of lift coefficient.

Comparison of Experimental and Estimated Retractable-Aileron Effectiveness

In order to determine whether the methods employed for estimating the characteristics of flap controls on unswept and sweptback wings (references 12 and 13) apply equally as well to spoiler ailerons on low-aspect-ratio wings, values of C_l produced by $0.60\frac{b}{2}$ retractable ailerons at a projection of -0.08c on unswept untapered wings having various aspect ratios and on the 45° sweptback wing of aspect ratio 2.09 for various aileron spanwise locations were estimated and are compared in figure 15 with experimental data obtained in the present investigation for $C_L = 0$. The estimated curves of figure 15 were computed by the following equation, which represents a modified version of the method presented in reference 13:

$$C_l = \frac{C_l}{\Delta\alpha}\,\Delta\alpha\,K_1K_2\cos^2\Lambda$$

The following terms of the foregoing equation are defined as

$C_l/\Delta\alpha$ rolling-moment coefficient caused by a unit change in effective angle of attack over part of wing span occupied by control surface

$\Delta\alpha$ change in effective angle of attack caused by retractable-aileron projection, degrees

K_1 aspect-ratio correction factor

K_2 taper-ratio correction factor

Values of $C_l/\Delta\alpha$ and K_2 used in the computations were obtained from reference 13. Experimentally determined values of K_1 (reference 11) were employed in these computations for all unswept wings having aspect ratios of 4 or less, and values of the aileron-effectiveness parameter ($\Delta\alpha$) of 7.6 and 9.5 (obtained from unpublished two-dimensional spoiler-control data) were used in the computations of C_l for the unswept and 45° sweptback wings, respectively.

The data of figure 15(a) show that the empirical method of reference 13 was reasonably accurate for estimating the effectiveness of the retractable ailerons on the unswept wings - particularly for the larger aspect ratios. The effectiveness of spoiler ailerons on the sweptback wing of aspect ratio of 2.09 was overestimated at all spanwise stations because of differences in the spanwise-effectiveness characteristics of the plain and stepped retractable ailerons and the poor agreement between experimental and estimated values of C_l (fig. 15(b)).

Rolling Performance

The low-aspect-ratio wings with retractable ailerons.- In order to illustrate the rolling effectiveness of the retractable-aileron configurations investigated, values of the wing-tip helix angle pb/2V were estimated for the unswept wings and also for the 45° sweptback wing (with the optimum plain- and stepped-retractable-aileron configurations). The estimated values of pb/2V were obtained from the relationship $\frac{pb}{2V} = \frac{C_l}{C_{l_p}}$, and the values of C_l used in this equation were for retractable ailerons having a projection of -0.08c. The values of C_{l_p} used for determining the values of pb/2V were obtained from the expression $C_{l_p} = \left(C_{l_p}\right)_{C_L=0} \frac{\left(C_{L_\alpha}\right)_{C_L}}{\left(C_{L_\alpha}\right)_{C_L=0}}$ presented as method 1 in reference 14 and are shown in figure 16. The values of $\left(C_{l_p}\right)_{C_L=0}$ used in the foregoing equation were -0.108, -0.195, and -0.330 for the unswept wings of aspect ratio 1.13, 2.13, and 4.13, respectively, and -0.190 for the 45° sweptback wing of aspect ratio 2.09 and were obtained from reference 15.

The estimated values of pb/2V (fig. 17) show that a wing-tip helix angle of 0.09 radian (an Air Force - Navy requirement) can usually be obtained with the retractable ailerons on the wing model of aspect

ratio 4.13. The retractable ailerons on the other wings, however, produced much lower values of $pb/2V$, inasmuch as the aileron rolling effectiveness generally decreased with decrease in wing aspect ratio and when the wing was sweptback. Furthermore, the rolling effectiveness of the ailerons on any of the models was rather erratic over the lift range.

Although the values of $pb/2V$ produced by the retractable ailerons on some of the wing models were not very large, their magnitude may not be of great importance. For an airplane having a given wing loading (or wing area), values of the rolling velocity p may be more indicative of good control than $pb/2V$, because of the shorter wing span and higher rolling velocities experienced by such an airplane at a given value of $pb/2V$ as the wing aspect ratio decreased. On this basis, the rolling velocities of the three unswept wings and the 45° sweptback wing with the optimum plain-retractable-aileron configuration are estimated to be approximately equal for an aileron projection of -0.08c and at the same speed.

Comparison of spoiler and flap ailerons on the low-aspect-ratio wings.- A comparison of the rolling effectiveness parameter $pb/2V$ of the retractable (spoiler) ailerons (obtained from fig. 17) and of the flap ailerons investigated on the same wings (estimated from C_l data of reference 11 and unpublished data) is shown in figure 18. The data presented in figure 18 for the flap ailerons are for 0.25c, half-span, outboard, sealed plain ailerons deflected 10° and -10° or a total of 20°. The same methods employed in computing the values of $pb/2V$ for the retractable ailerons and discussed in the preceding section of the present paper were employed for the flap ailerons.

Both types of ailerons produced similar trends in the variation of $pb/2V$ over the lift range (fig. 18). The half-span flap ailerons deflected a total of 20° were more effective than the spoiler ailerons projected -0.08c on the same wings, except for a limited range of lift coefficients on the 45° sweptback-wing model. The following table shows the estimated span of 0.25c flap ailerons deflected a total of 20° that would generally equal the rolling effectiveness of a $0.60\frac{b}{2}$ retractable aileron $\left(\frac{y_1}{b/2} = 0.40\right)$ projected -0.08c on each of the wings:

A	Λ (deg)	Estimated span of flap ailerons to produce same pb/2V as $0.60\frac{b}{2}$ retractable ailerons (percent b/2)
1.13	0	23
2.13	0	30
4.13	0	38
2.09	45	[a]45

[a]Comparison made with optimum plain retractable aileron, $\frac{y_i}{b/2} = 0$.

The data given in the previous table, as well as the data of figure 18, show that retractable ailerons on low-aspect-ratio unswept wings are rather ineffective when compared with reasonably normal-size flap ailerons and become progressively worse as the wing aspect ratio is decreased.

Such a comparison is rather incomplete, however, when the effects of the aileron yawing moments, of the aileron hinge moments, and of compressibility are not considered. In general, the yawing moments of spoiler ailerons are favorable and would tend to increase the rolling effectiveness of these controls as contrasted to opposite effects exhibited by the flap ailerons at high angles of attack. The data of references 2 and 3 show that the spoiler ailerons were more effective than the flap ailerons when compressibility effects were considered, and, in addition, reference 8 indicates that the twist of the wing with spoiler controls was less than that of the wing with flap controls.

CONCLUSIONS

A low-speed wind-tunnel investigation was made to determine the lateral control characteristics of three untapered unswept wings of aspect ratio 1.13, 2.13, and 4.13 and an untapered 45° sweptback wing of aspect ratio 2.09 equipped with 0.60-semispan retractable ailerons having various projections. The ailerons investigated on the unswept wings spanned the outboard stations of each wing; whereas the plain and stepped retractable ailerons investigated on the sweptback wing were located at various spanwise stations. The results of the investigation led to the following conclusions:

1. At equal aileron projections, the rolling effectiveness of the retractable ailerons increased with increase in aspect ratio of the unswept wings and decreased with increase in wing sweepback; however, the rolling velocities produced on the four wings are estimated to be approximately equal for a given wing area (or wing loading) at the maximum aileron projection investigated.

2. The effectiveness of plain retractable ailerons on the 45° sweptback wing generally increased when the spanwise location of the aileron was moved inboard; whereas the effectiveness of stepped retractable ailerons on the same wing generally increased at low and moderate angles of attack when their spanwise location was moved outboard. The optimum configuration for the plain retractable aileron (at the inboard location) was usually more effective than the optimum configuration for the stepped retractable aileron (at the outboard location) on the sweptback wing.

3. The addition of simulated actuating arms to the plain and stepped retractable ailerons investigated at various spanwise locations on the sweptback wing generally tended to increase the aileron effectiveness.

4. In general, the values of yawing-moment coefficient C_n produced by the ailerons on the four wings were favorable and increased linearly with aileron projection except at small projections.

5. The effectiveness of the retractable ailerons on the unswept wings could be predicted by an existing empirical method for low angles of attack; however, this empirical method tended to overestimate the effectiveness of retractable ailerons at all spanwise stations on the 45° sweptback wing.

Langley Aeronautical Laboratory
National Advisory Committee for Aeronautics
Langley Field, Va., January 2, 1951

REFERENCES

1. Fischel, Jack, and Tamburello, Vito: Investigation of Effect of Span, Spanwise Location, and Chordwise Location of Spoilers on Lateral Control Characteristics of a Tapered Wing. NACA TN 1294, 1947.

2. Fischel, Jack, and Schneiter, Leslie E.: High-Speed Wind-Tunnel Investigation of an NACA 65-210 Semispan Wing Equipped with Plug and Retractable Ailerons and a Full-Span Slotted Flap. NACA TN 1663, 1948.

3. Laitone, Edmund V., and Summers, James L.: An Additional Investigation of the High-Speed Lateral-Control Characteristics of Spoilers. NACA ACR 5D28, 1945.

4. Fischel, Jack, and Ivey, Margaret F.: Collection of Test Data for Lateral Control with Full-Span Flaps. NACA TN 1404, 1948.

5. Schneiter, Leslie E., and Watson, James M.: Low-Speed Wind-Tunnel Investigation of Various Plain-Spoiler Configurations for Lateral Control on a 42° Sweptback Wing. NACA TN 1646, 1948.

6. Lovell, Powell M., Jr., and Stassi, Paul P.: A Comparison of the Lateral Controllability with Flap and Plug Ailerons on a Sweptback-Wing Model. NACA TN 2089, 1950.

7. Lovell, Powell M., Jr.: A Comparison of the Lateral Controllability with Flap and Plug Ailerons on a Sweptback-Wing Model Having Full-Span Flaps. NACA TN 2247, 1950.

8. Purser, Paul E., and McKinney, Elizabeth G.: Comparison of Pitching Moments Produced by Plain Flaps and by Spoilers and Some Aerodynamic Characteristics of an NACA 23012 Airfoil with Various Types of Aileron. NACA ACR L5C24a, 1945.

9. Gillis, Clarence L., Polhamus, Edward C., and Gray, Joseph L., Jr.: Charts for Determining Jet-Boundary Corrections for Complete Models in 7- by 10-Foot Closed Rectangular Wind Tunnels. NACA ARR L5G31, 1945.

10. Herriot, John G.: Blockage Corrections for Three-Dimensional-Flow Closed-Throat Wind Tunnels, with Consideration of the Effect of Compressibility. NACA Rep. 995, 1950. (Formerly NACA RM A7B28.)

11. Naeseth, Rodger L., and O'Hare, William M.: Effect of Aspect Ratio on the Low-Speed Lateral Control Characteristics of Unswept Untapered Low-Aspect-Ratio Wings. NACA TN 2348, 1951.

12. Weick, Fred E., and Jones, Robert T.: Résumé and Analysis of N.A.C.A. Lateral Control Research. NACA Rep. 605, 1937.

13. Lowry, John G., and Schneiter, Leslie E.: Estimation of Effectiveness of Flap-Type Controls on Sweptback Wings. NACA TN 1674, 1948.

14. Goodman, Alex, and Adair, Glenn H.: Estimation of the Damping in Roll of Wings through the Normal Flight Range of Lift Coefficient. NACA TN 1924, 1949.

15. Polhamus, Edward C.: A Simple Method of Estimating the Subsonic Lift and Damping in Roll of Sweptback Wings. NACA TN 1862, 1949.

TABLE I.- GEOMETRIC CHARACTERISTICS OF THE WING MODELS TESTED

[Each of the wing models had an NACA 64A010 airfoil section normal to the wing leading edge.]

Aspect ratio, A	Sweep, Λ (deg)	Span, b (ft)	Chord, c (ft)	Mean aerodynamic chord, $\bar{c}$ (ft)	Area, S (sq ft)
4.13	0	5.021	1.224	1.221	6.097
2.13	0	3.637	1.732	1.714	6.199
1.13	0	2.693	2.448	2.409	6.394
2.09	45	3.586	1.732	1.718	6.154

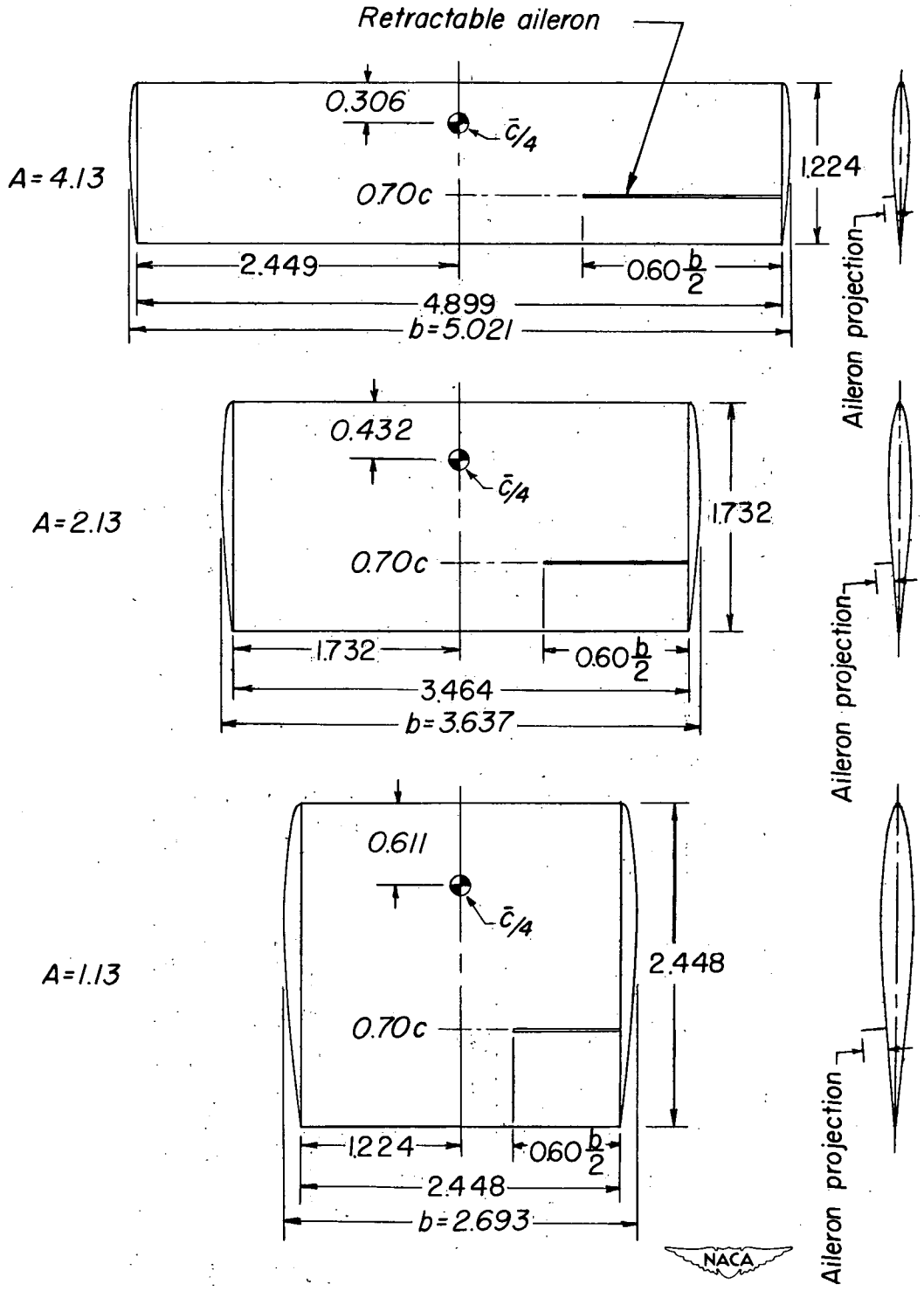

Figure 1.- Geometric characteristics of the unswept untapered wings investigated with retractable ailerons. (All dimensions in feet except where noted.)

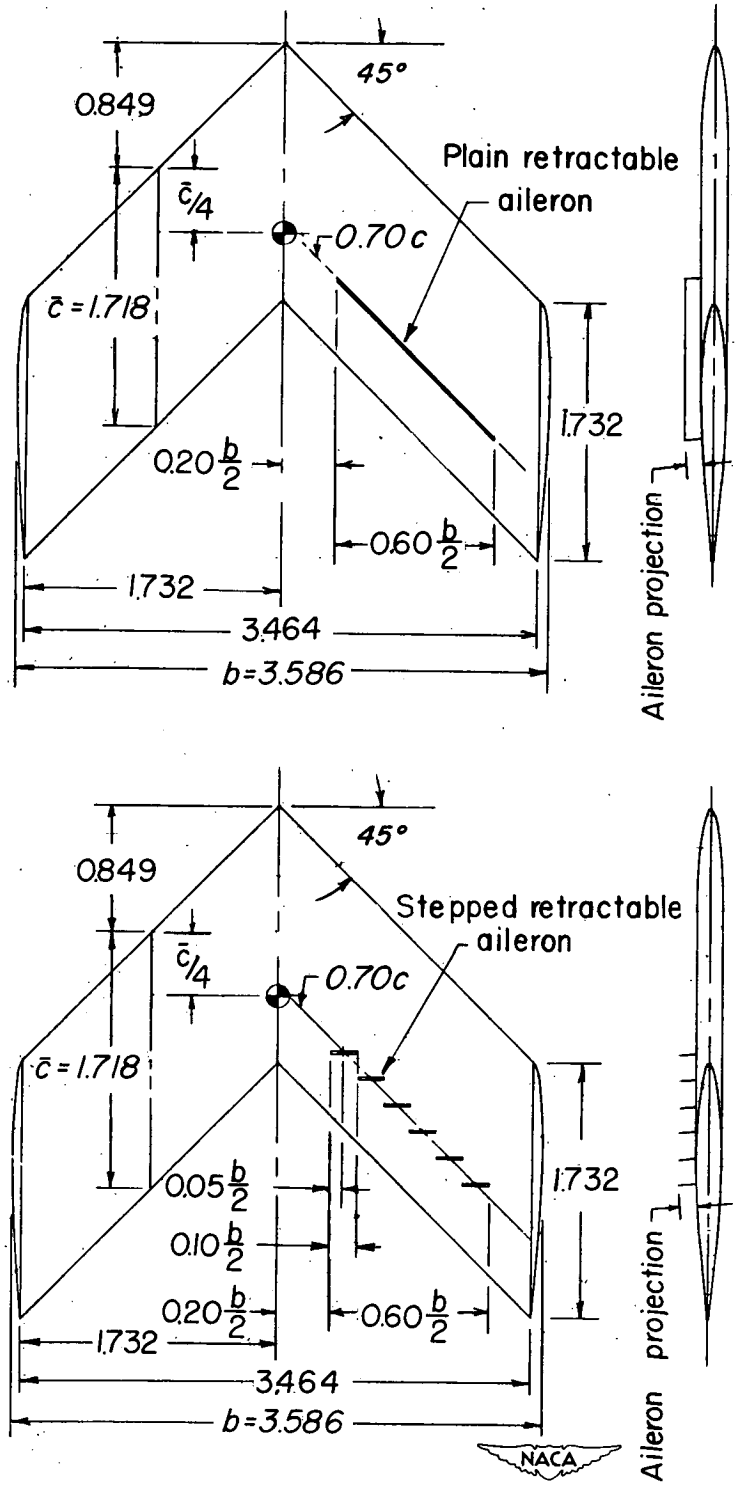

Figure 2.- Geometric characteristics of the 45° sweptback untapered wing investigated with plain and stepped retractable ailerons. A = 2.09. (All dimensions in feet except where noted.)

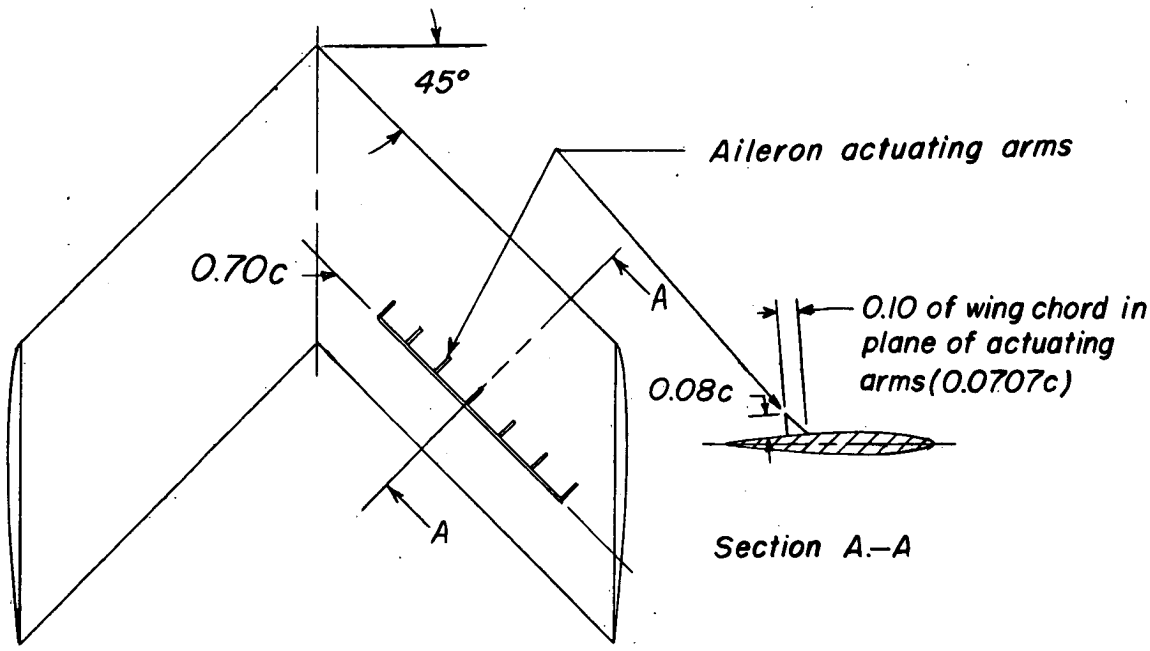

(a) Plain-retractable-aileron configuration.

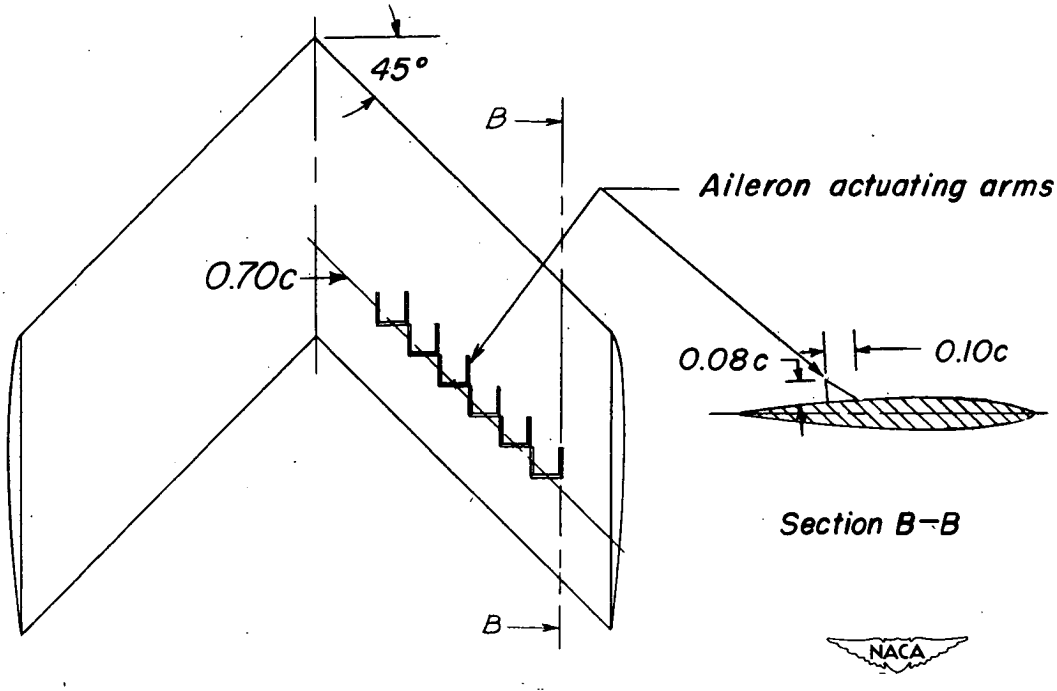

(b) Stepped-retractable-aileron configuration.

Figure 3.- Geometric characteristics of the plain and stepped retractable ailerons tested with aileron actuating arms on the 45° sweptback wing of aspect ratio 2.09. $b_a = 0.60\frac{b}{2}$.

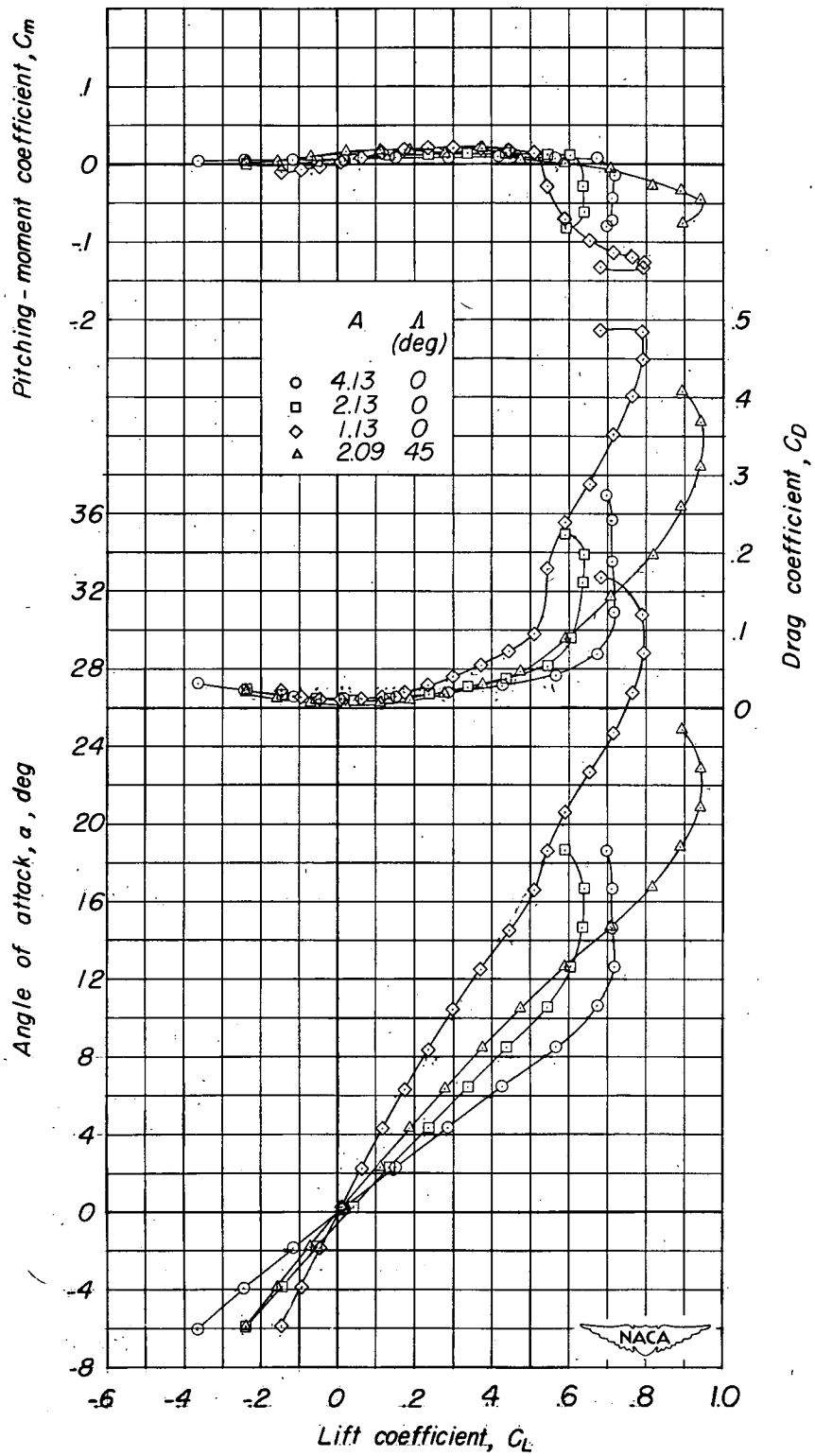

Figure 4.- Aerodynamic characteristics in pitch of the plain unswept and 45° sweptback untapered wings investigated.

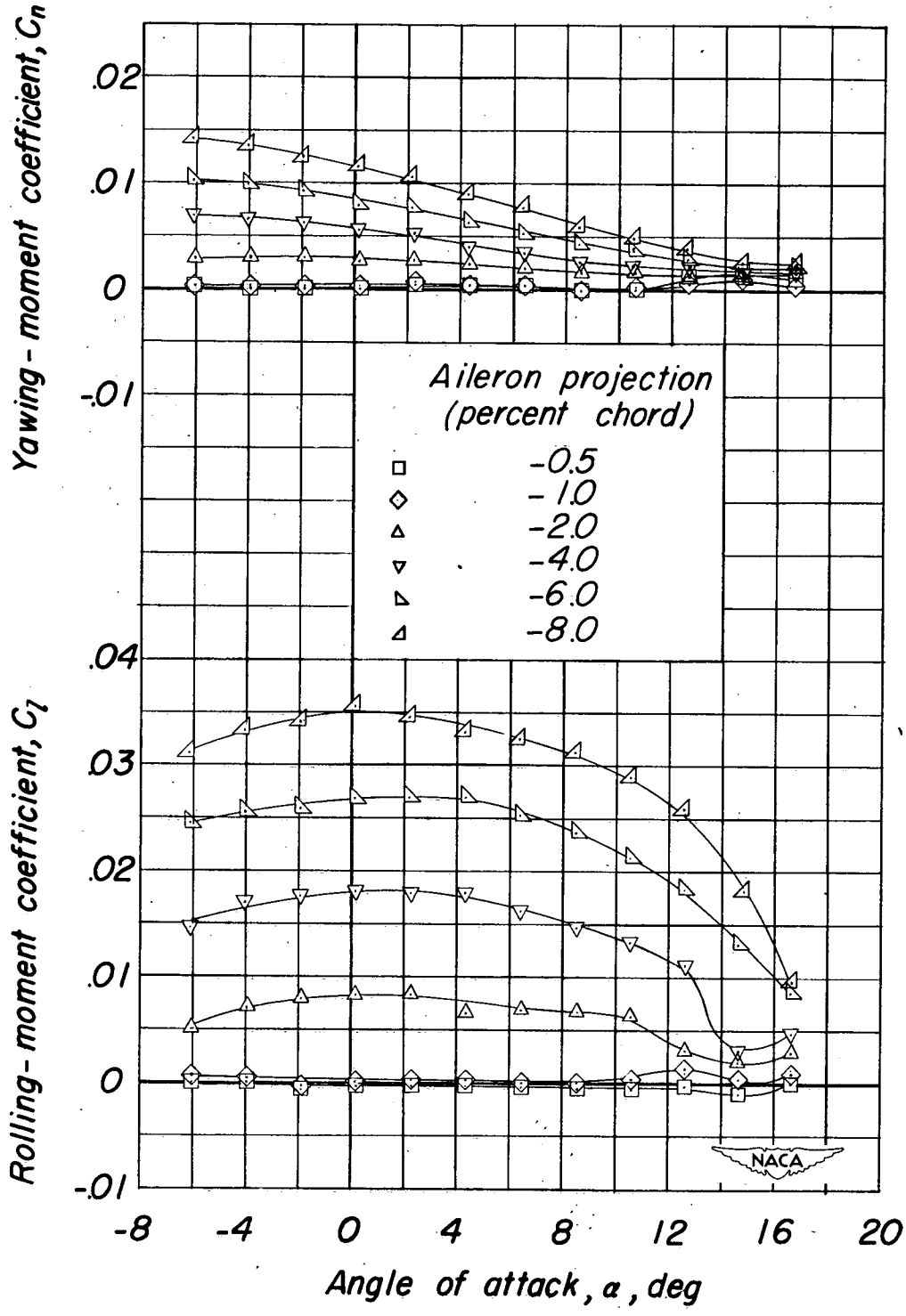

Figure 5.- Variation of lateral control characteristics with angle of attack of the unswept untapered wing of aspect ratio 4.13 equipped with retractable ailerons. $b_a = 0.60\frac{b}{2}$.

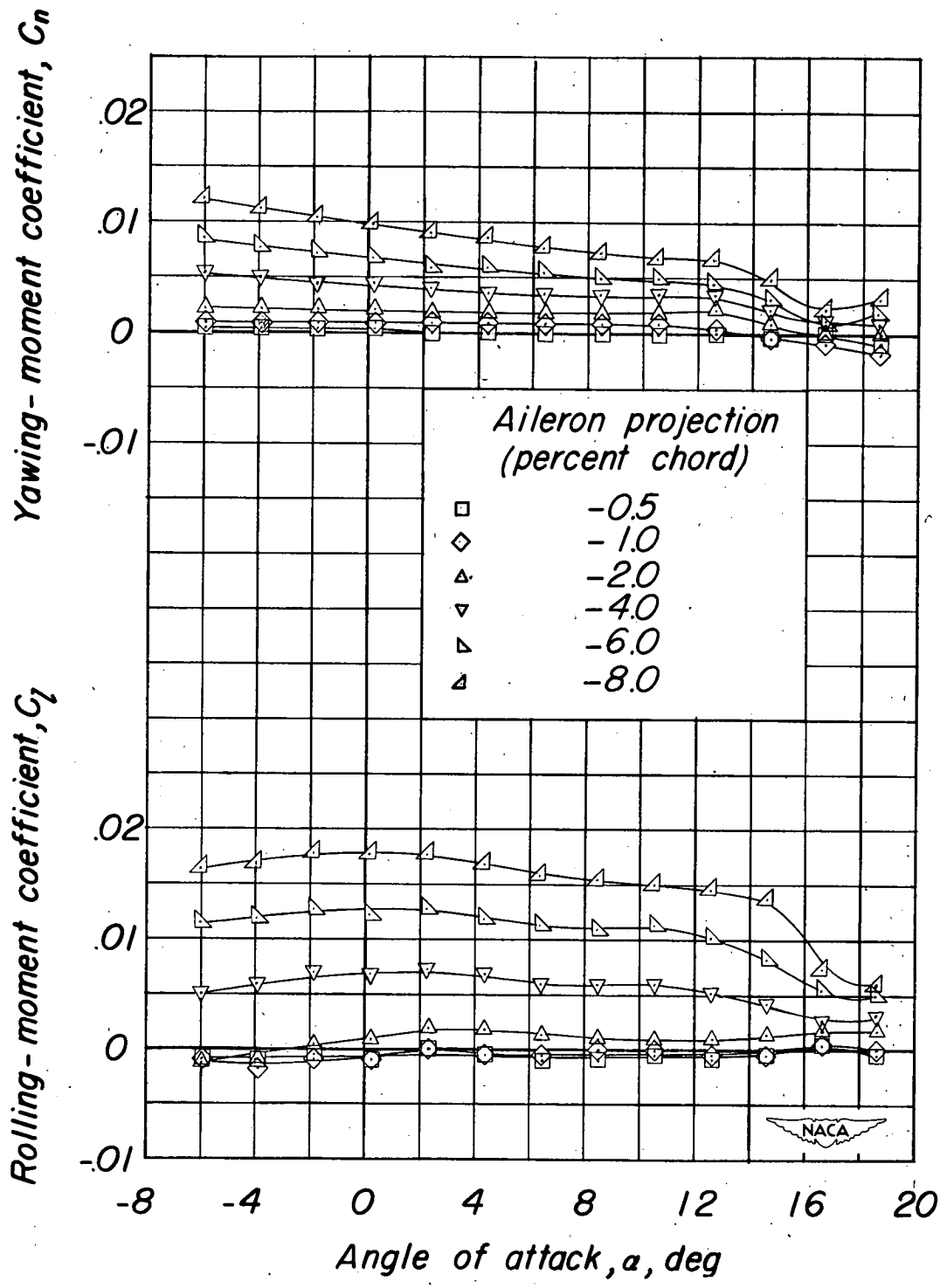

Figure 6.- Variation of lateral control characteristics with angle of attack of the unswept untapered wing of aspect ratio 2.13 equipped with retractable ailerons. $b_a = 0.60\frac{b}{2}$.

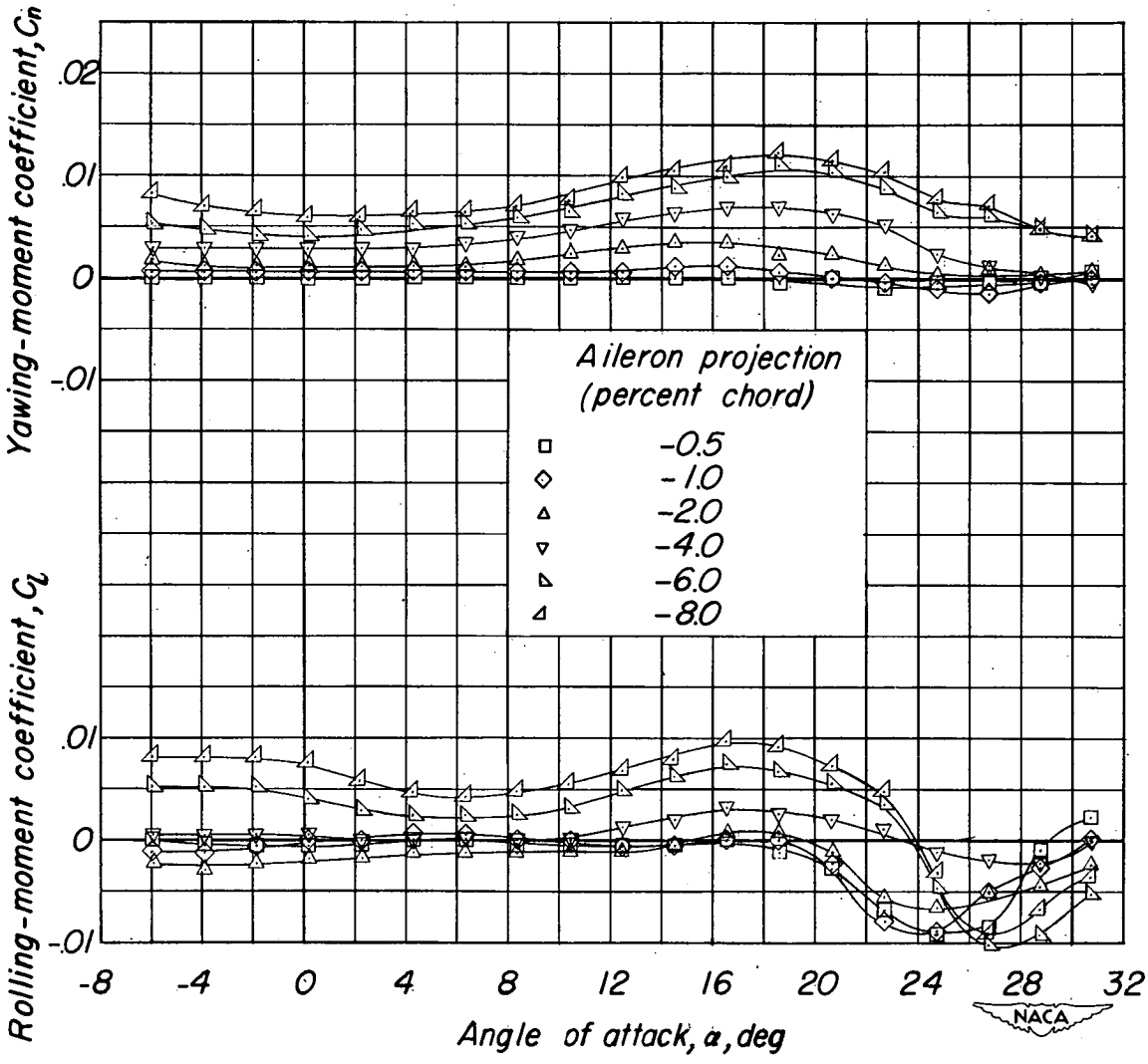

Figure 7.- Variation of lateral control characteristics with angle of attack of the unswept untapered wing of aspect ratio 1.13 equipped with retractable ailerons. $b_a = 0.60\frac{b}{2}$.

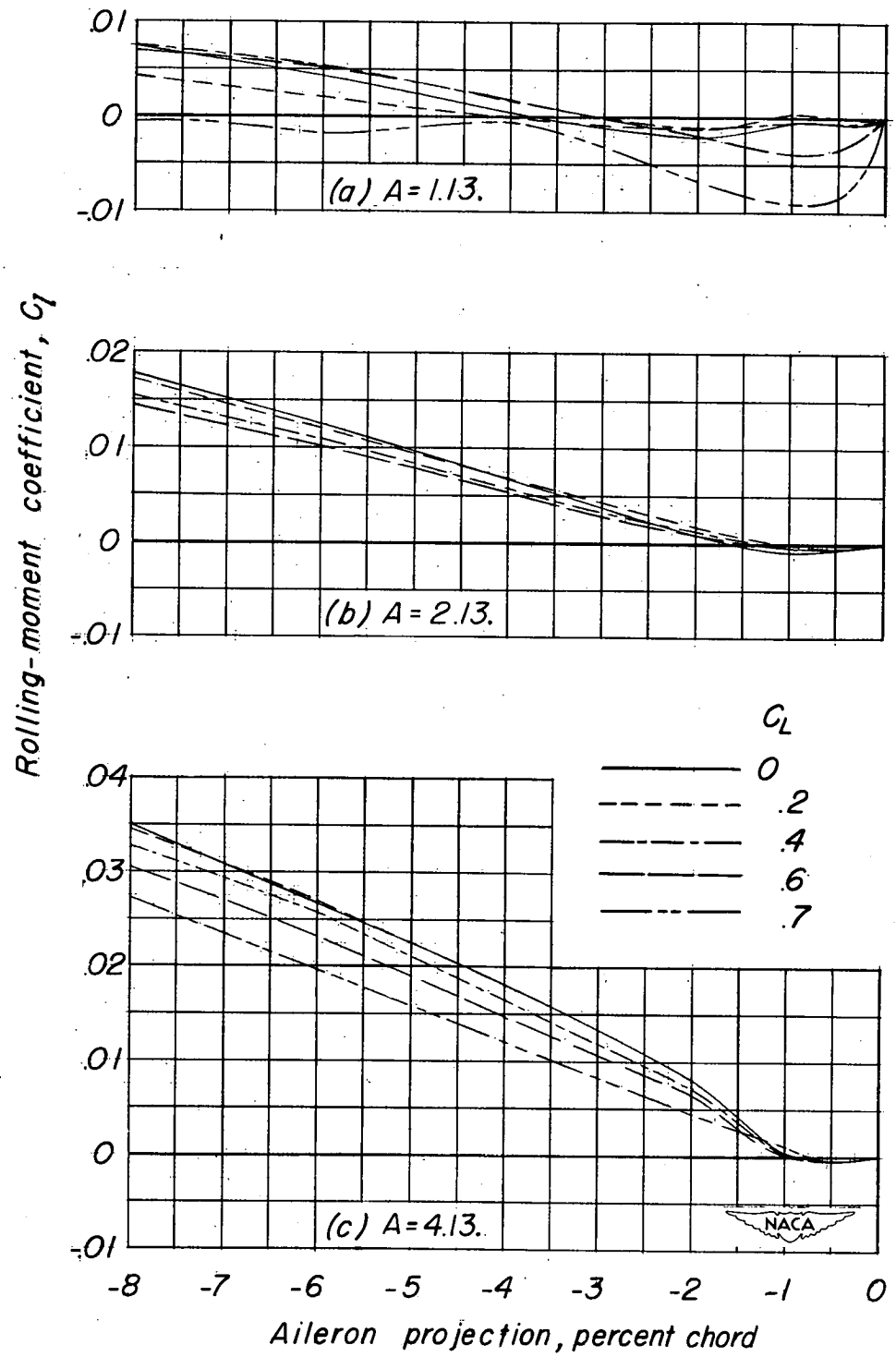

Figure 8.- Variation of rolling-moment coefficient with retractable-aileron projection on the unswept untapered wings investigated. $b_a = 0.60\frac{b}{2}$.

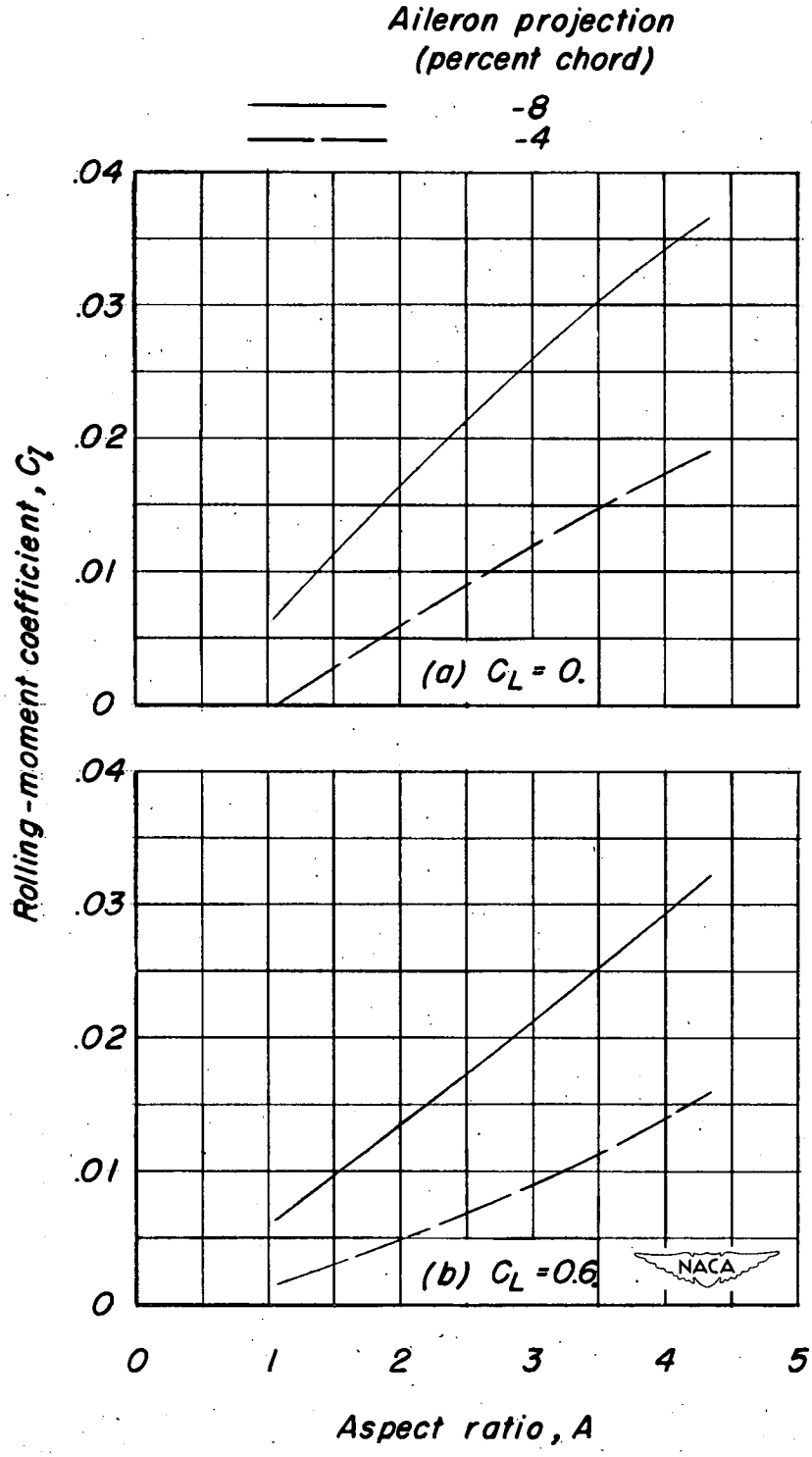

Figure 9.- Effect of wing aspect ratio on the rolling-moment characteristics of the unswept untapered wings. $b_a = 0.60\frac{b}{2}$.

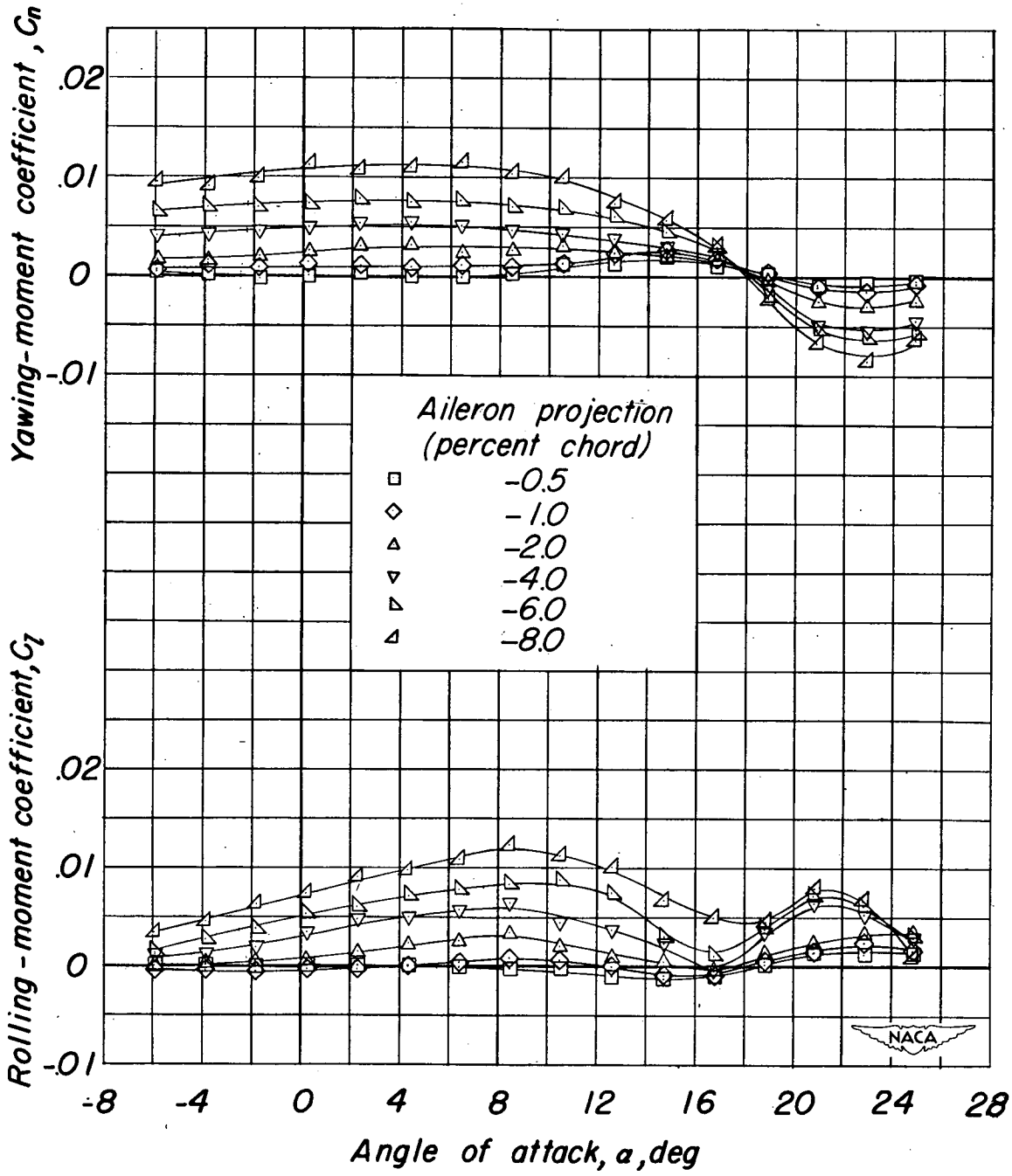

Figure 10.- Variation of lateral control characteristics with angle of attack of the 45° sweptback untapered wing of aspect ratio 2.09 equipped with plain retractable ailerons. $b_a = 0.60\frac{b}{2}$; $y_i = 0.20\frac{b}{2}$.

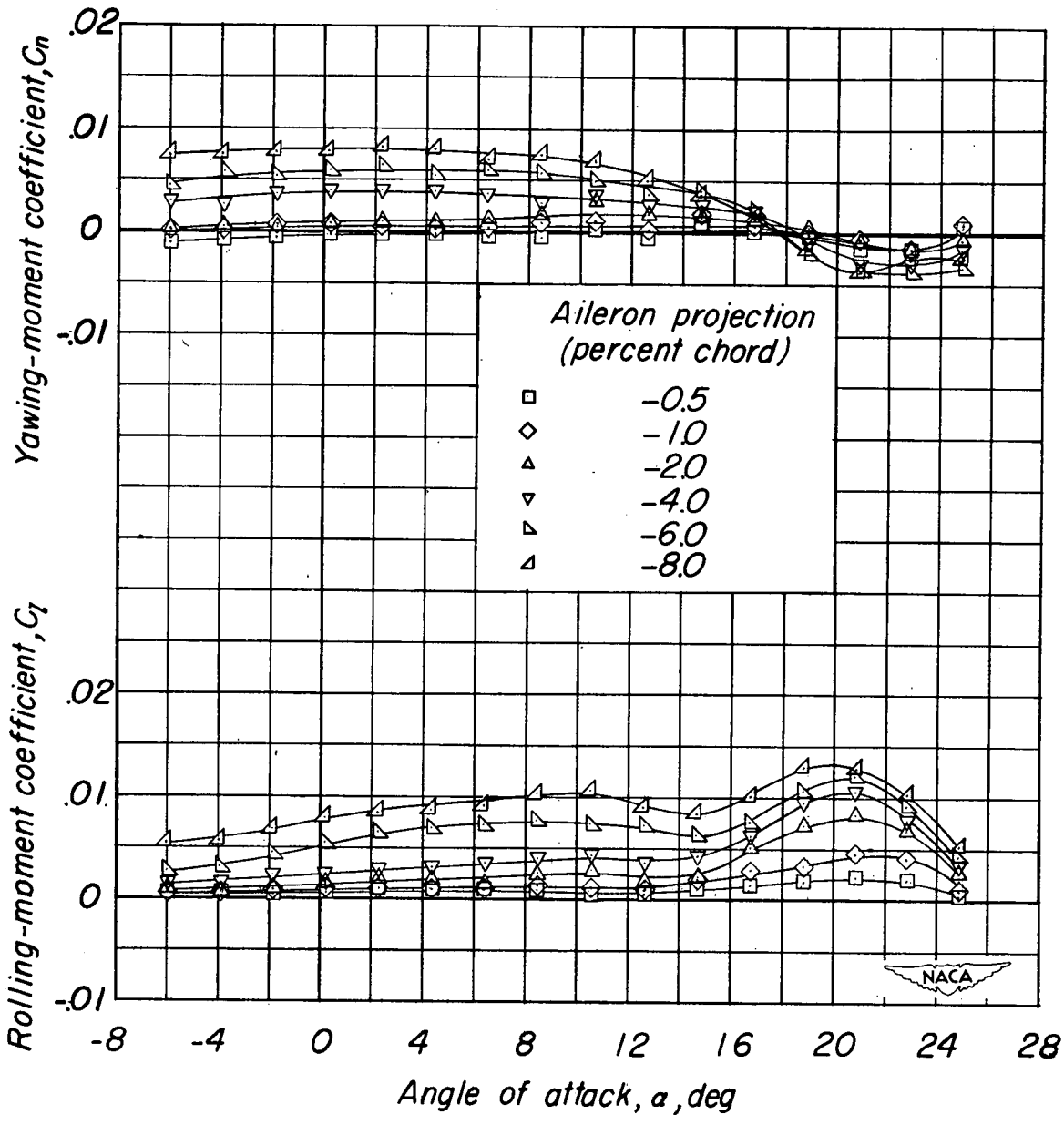

Figure 11.- Variation of lateral control characteristics with angle of attack of the 45° sweptback untapered wing of aspect ratio 2.09 equipped with stepped retractable ailerons. $b_a = 0.60\frac{b}{2}$; $y_1 = 0.20\frac{b}{2}$.

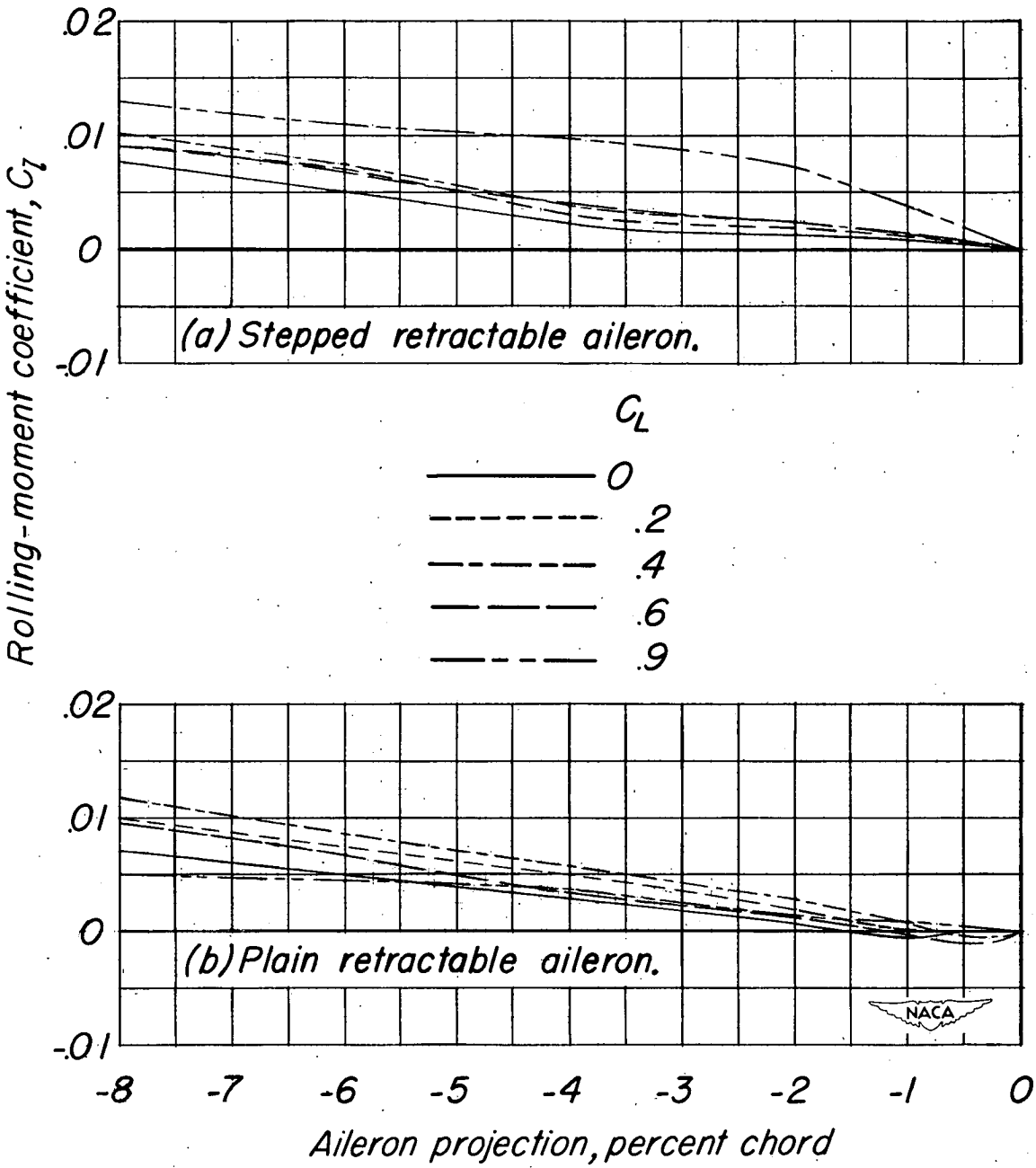

Figure 12.- Variation of rolling-moment coefficient with retractable-aileron projection on the 45° sweptback untapered wing of aspect ratio 2.09. $b_a = 0.60\frac{b}{2}$; $y_1 = 0.20\frac{b}{2}$.

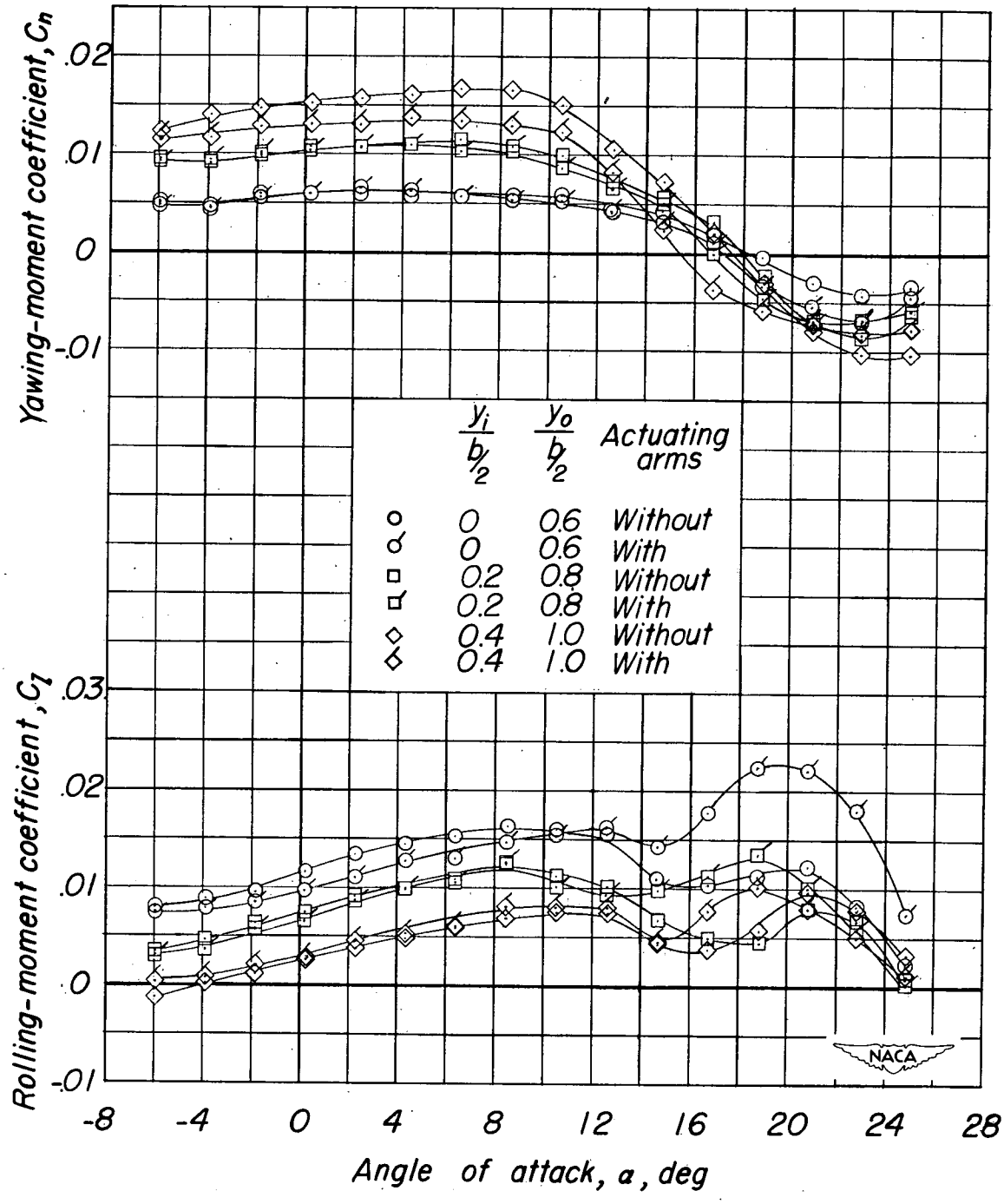

Figure 13.- Effect of aileron spanwise location and aileron actuating arms on the lateral control characteristics of the 45° sweptback untapered wing of aspect ratio 2.09 equipped with plain retractable ailerons. Aileron projection, -0.08c; $b_a = 0.60\frac{b}{2}$.

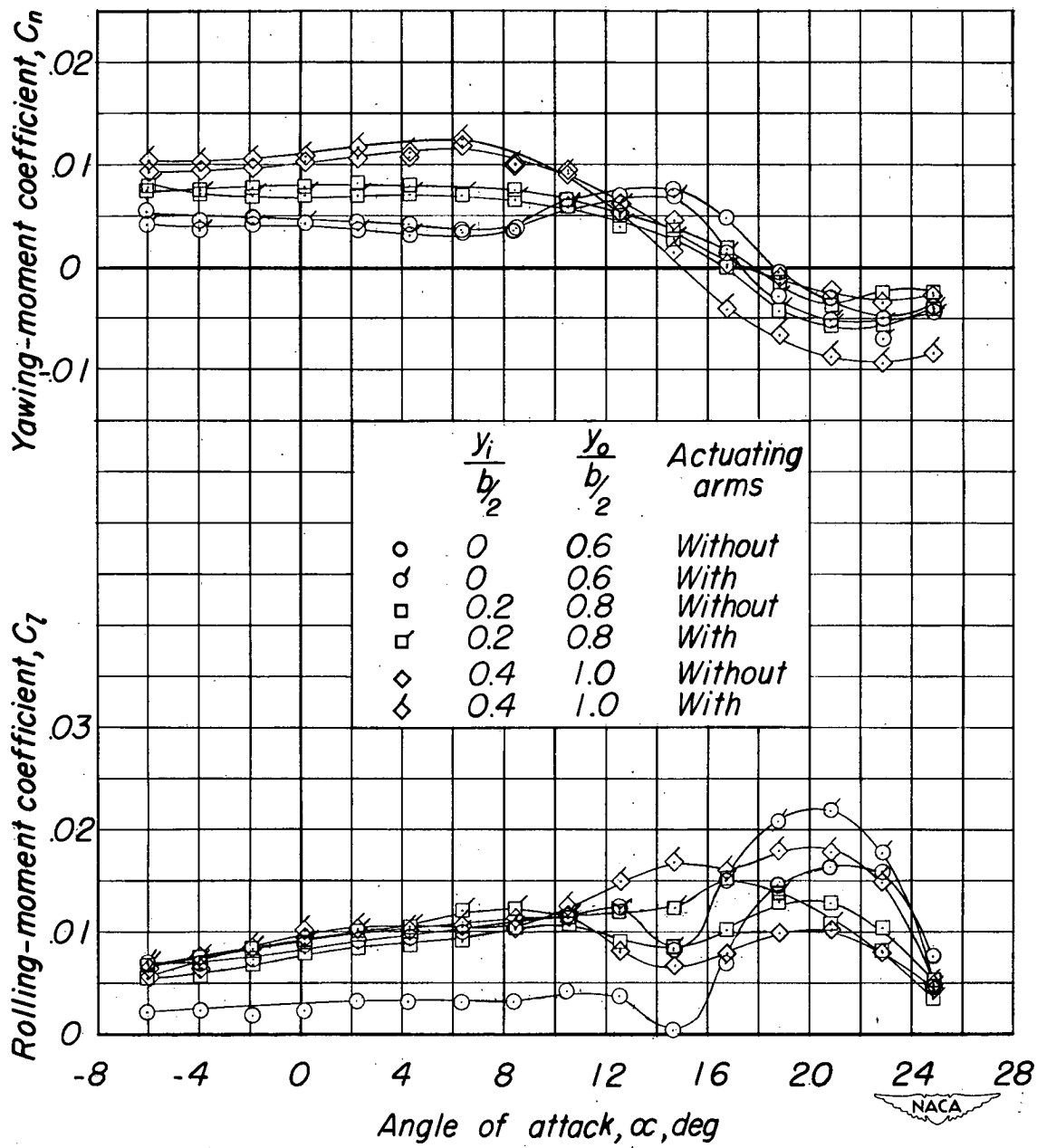

Figure 14.- Effect of aileron spanwise location and aileron actuating arms on the lateral control characteristics of the 45° sweptback untapered wing of aspect ratio 2.09 equipped with stepped retractable ailerons. Aileron projection, -0.08c; $b_a = 0.60\frac{b}{2}$.

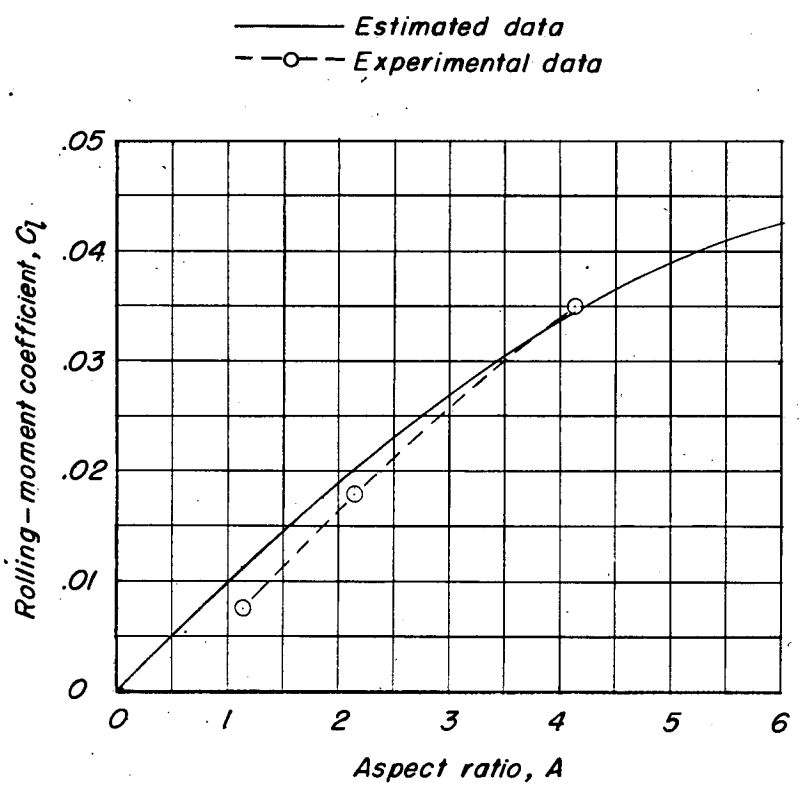

(a) $\Lambda = 0^\circ$; $\frac{y_i}{b/2} = 0.30$ to 0.40.

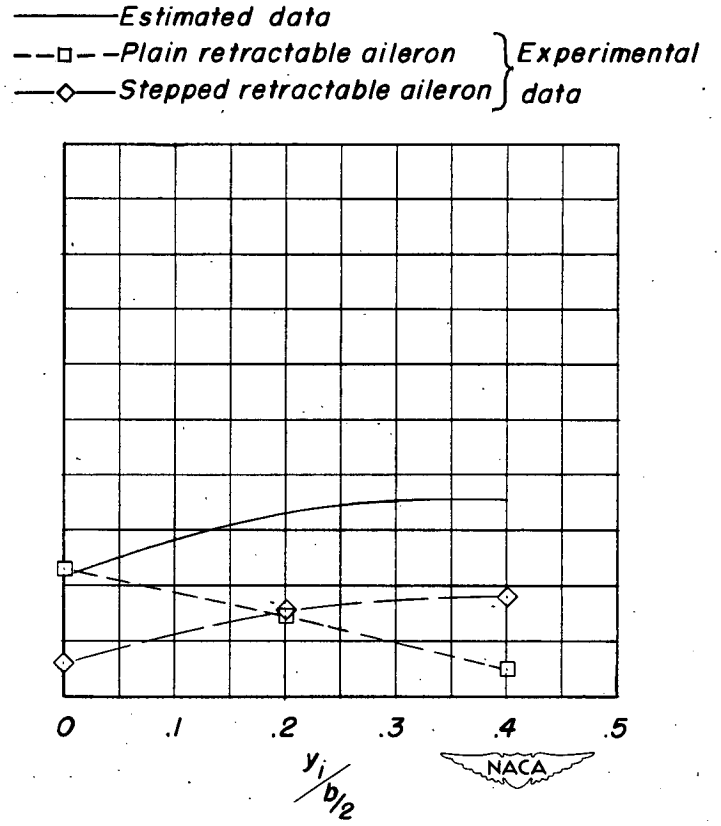

(b) $\Lambda = 45^\circ$; A = 2.09.

Figure 15.- Comparison of experimental and estimated values of C_l for $0.60\frac{b}{2}$ retractable ailerons at a projection of -0.08c on the untapered wings. $C_L = 0$.

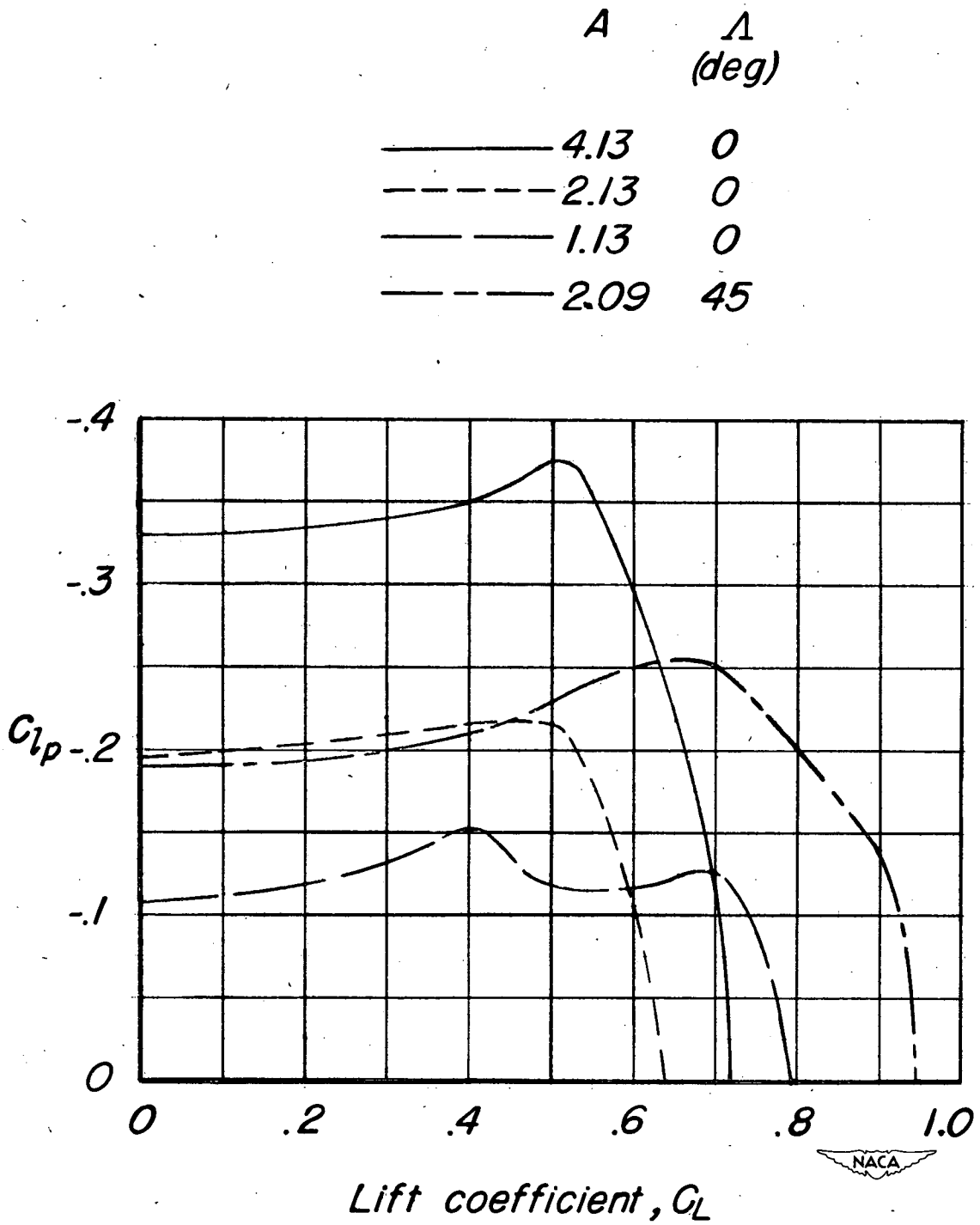

Figure 16.- Variation of C_{l_p} $\left(\text{used for determining } \frac{pb}{2V}\right)$ with lift coefficient of the wings investigated.

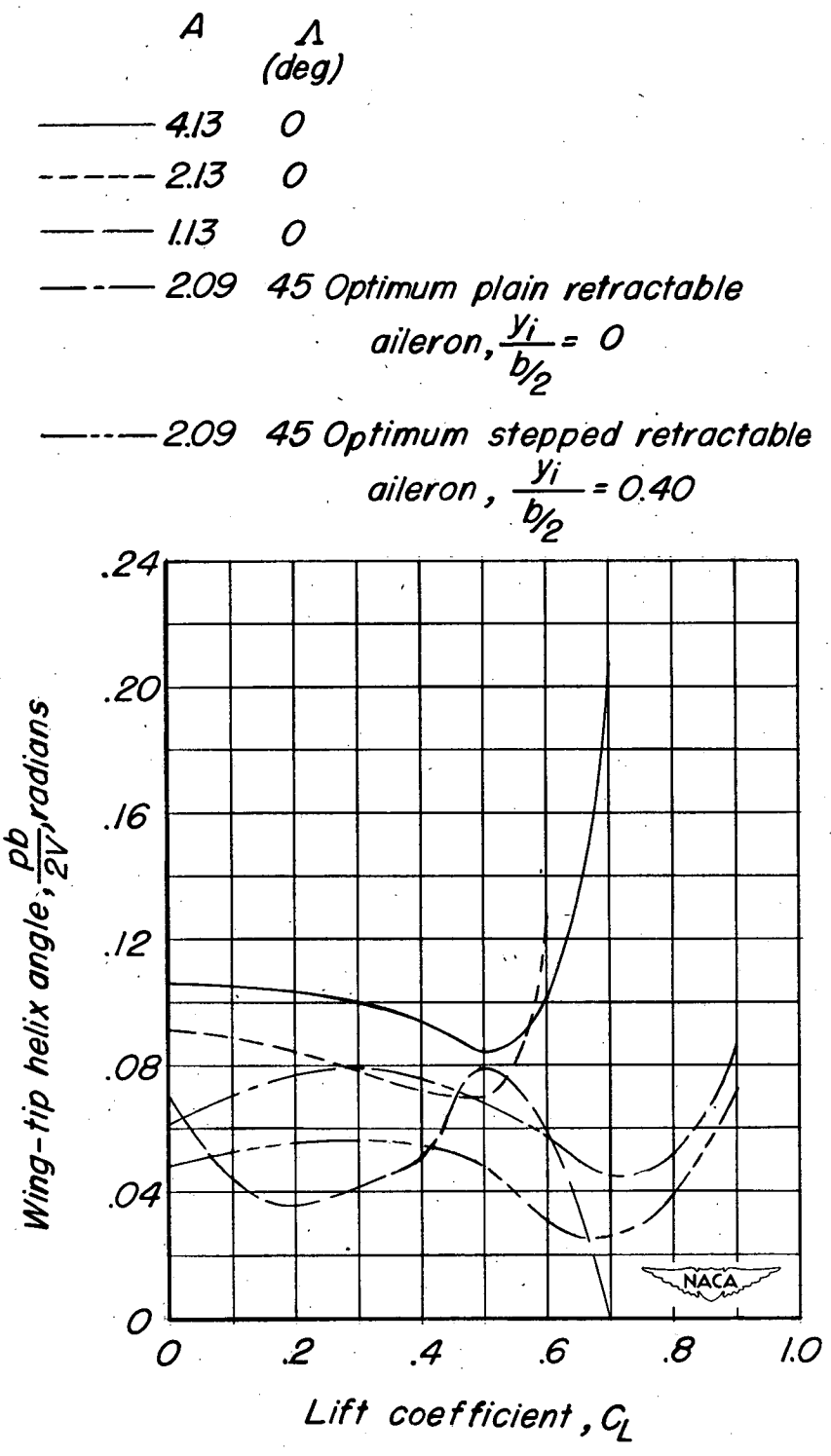

Figure 17.- Variation of estimated wing-tip helix angle with lift coefficient for the four wing models equipped with retractable ailerons.

$b_a = 0.60\frac{b}{2}$; aileron projection, -0.08c.

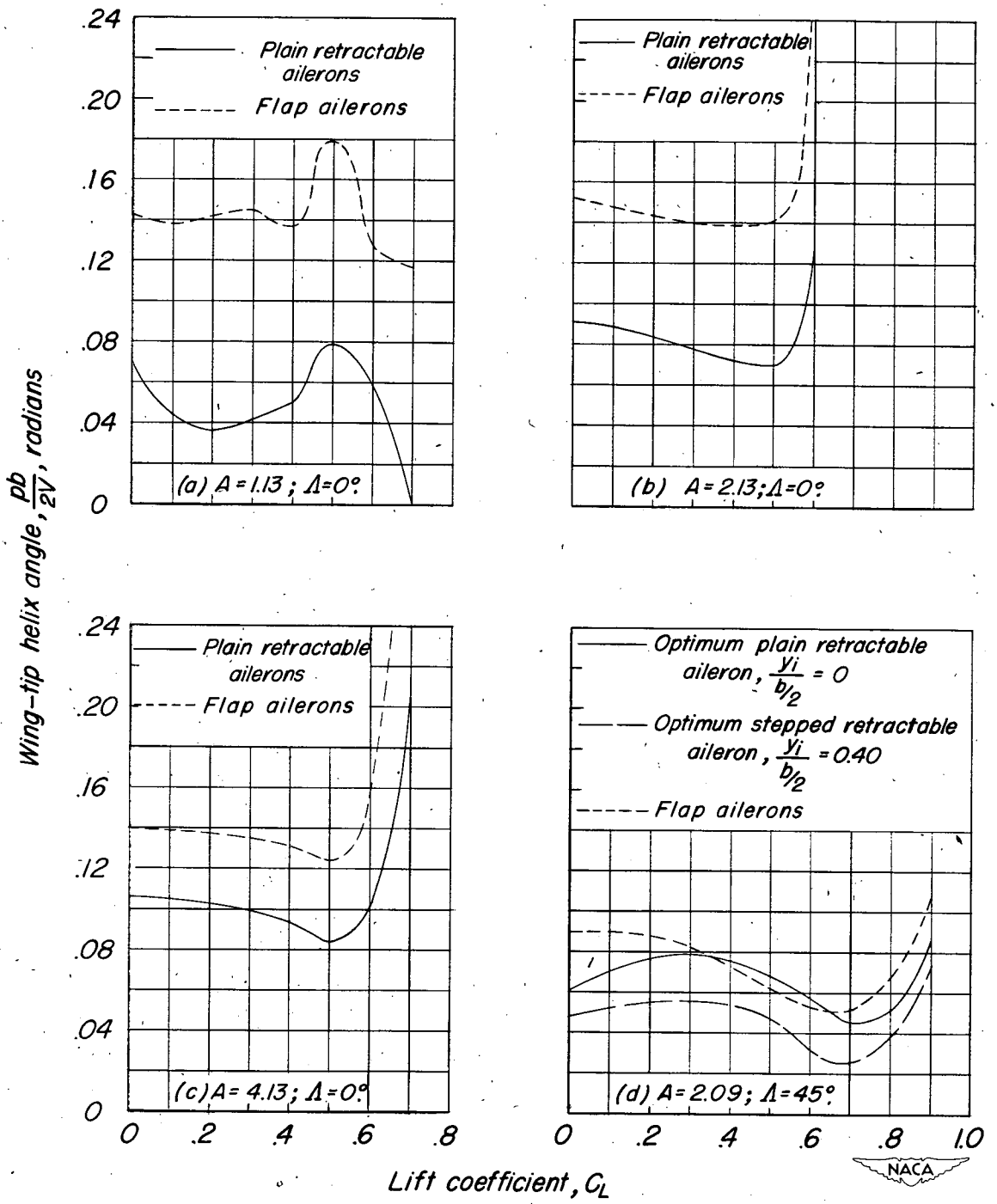

Figure 18.- Comparison of estimated values of $\frac{pb}{2V}$ produced by $0.60\frac{b}{2}$ retractable ailerons projected -0.08c and by half-span 0.25c sealed flap-ailerons deflected a total of 20° on each of the untapered low-aspect-ratio wings. (Flap-aileron data were estimated from C_l data of reference 11 and unpublished data.)